Discrete Comput Geom (2010) 43: 855–875
DOI 10.1007/s00454-009-9211-1

The Finite Number of Interior Component Shapes of the Levy Dragon

Eytan Alster

Received: 11 November 2008 / Revised: 22 June 2009 / Accepted: 25 June 2009 /
Published online: 11 July 2009

Abstract The Levy dragon is a connected self-similar tile with disconnected interior. It was previously known that there are at least 16 different shapes of its interior components. Using simple properties of an infinite sequence of curves which converge into the Levy dragon, it is proved that the number of different shapes of the interior components is finite. A detailed description of the buildup of those shapes as unions of various contractions of three convex polygonal shapes is given, and the number of shapes is determined.

Keywords Levy dragon · Interior component shapes

1 Introduction

The Levy dragon K (Fig. 1) is the attractor of an iterated function system $F = \{f_0, f_1\}$ where the two $\mathbb{R}^2 \to \mathbb{R}^2$ contracting similarity transformations f_0 and f_1 include contraction by $1/\sqrt{2}$ and a rotation by $\pi/4$ for f_0 and by $-\pi/4$ for f_1. As proved by Huchinson [5], the attractor of such a system is a unique compact set that satisfies

$$K = f_0(K) \cup f_1(K)$$

For any compact set S, let $F(S) = f_0(S) \cup f_1(S)$; then $K = F(K)$, so K is the fixed point of F, and

$$K = \lim_{k \to \infty} F^k(S)$$

If S is a straight line segment C_0 whose end points are the fixed points of f_0 and f_1, the curves $C_k = F^k(C_0)$ converge (with respect to the Hausdorff metric) as $k \to \infty$

E. Alster (✉)
Hayarden 45, Ramat Gan 52271, Israel
e-mail: ealster@hotmail.com

Fig. 1 The Levy dragon

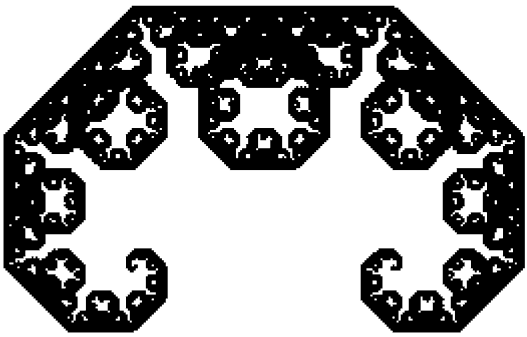

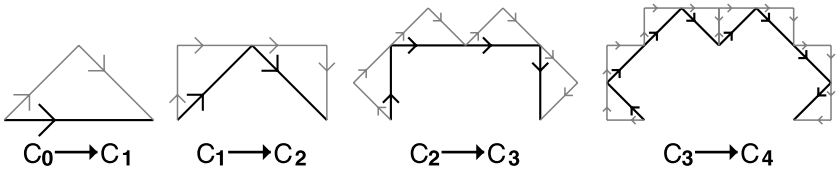

Fig. 2 First C_k curves iterations

to K. C_k consists of 2^k segments of length $l_k = (1/\sqrt{2})^k l_0$, where l_0 is the distance between the fixed points of f_0 and f_1. Figure 2 demonstrates the first iterations in this sequence with a curve in black and its next iteration in gray. Every C_k segment has a direction starting with the direction of C_0 from the fixed point of f_0 to the fixed point of f_1. C_{k+1} is obtained from C_k by replacing every segment of C_k by two segments that form with it an isosceles right triangle with the C_k segment its hypotenuse and the triangle to the left with respect to its direction. The directions of the two C_{k+1} segments replacing a C_k segment are such that they form a path from its start to its end. For the rest of this paper, a C_k segment means a directed segment as marked by the arrows in Fig. 2. When there are two opposite arrows on the same segment as for one of the segments in C_4, there are two overlapping segments with opposite directions. Properties of the curves C_k are discussed in Sect. 2.

Another choice for S used in many treatments of the Levy dragon is the isosceles right triangle T with end points of the hypotenuse at the fixed points of f_0 and f_1 and the third vertex to the left with respect to the direction from the fixed point of f_0 to the fixed point of f_1. That third vertex is the only common point of the two contracted triangles in $F(T)$, and their hypotenuses are on two sides of T (Fig. 3(a)). The 2^k contracted triangles in $F^k(T)$ are connected, but their interiors never overlap since, as demonstrated in Fig. 3(b), for any square with up to four $F^k(T)$ triangles, the $F^{k+1}(T)$ triangles that replace them are within that square, and their interiors do not overlap.

These two choices for S are thus related: the hypotenuses of the $F^k(T)$ triangles are the C_k segments, while their other two sides are the C_{k+1} segments. In this paper properties of the curves C_k are used through their relation to the $F^k(T)$ triangles to determine the shapes of the interior components of the Levy dragon in Sect. 3.

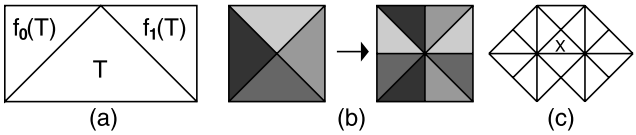

Fig. 3 (**a**) Triangle T and its two contractions $f_0(T)$ and $f_1(T)$. (**b**) Four triangles in a square and their next iteration. (**c**) A covered triangle

A similar method was used by Ngai and Nguyen [7] to prove geometric properties of the Heighway dragon using properties of the dragon curves.

P. Levy introduced in 1938 [6] (annotated English translation in [4]) the set now known as the Levy dragon as the limit of the sequence of curves C_k within a discussion of the properties of self similar curves like the Koch curve. Many properties of the Levy dragon are proved in [6]. Among them the location and shape of the largest of the interior components that consists of 22 triangles of $F^{16}(T)$ hence covers $22/2^{16} \approx 1/3000$ of the area of the Levy dragon, which is equal to the area of triangle T.

The Hausdorff dimension of the boundary of the Levy dragon was first calculated by Duvall and Keesling [2] to be $D = 1.934007183\ldots$. This dimension was calculated by Strichartz and Wang [9] using a different method.

Deng and Ngai [3] calculated the dimensions of subsets of the boundary of the Levy dragon which are the common intersection of at least a given number of neighbors in the tiling of the plane by copies of the Levy dragon. Ngai and Tang [8] proved that the closure of each interior component of the Levy dragon is a topological disk.

An $F^k(T)$ triangle with all the 14 triangles intersecting it also in $F^k(T)$, as demonstrated in Fig. 3(c) for triangle X there, is called in [2] *covered* since it is tiled by two $F^{k+1}(T)$ covered triangles and thus is a subset of K.

The Levy dragon is a connected set with disconnected interior. Bailey, Kim, and Strichartz [1] showed that contrary to the dragon boundary being a fractal, each of the infinitely many interior components, which are all too small to be seen in Fig. 1, has a one-dimensional polygonal boundary. By using a computer program that acts as a "microscope" into $F^k(T)$ and differentiates between an $F^k(T)$ triangle that is covered or not, the buildup of the interior components is observed. Covered triangles appear for the first time in $F^{14}(T)$, and following the growth of connected sets of covered triangles, they observed that distinct sets of covered triangles never merge and that some covered sets of triangles stop growing after a few iterations while other sets never stop growing. They identified 16 shapes of interior components and conjectured that each interior component is similar to one of those shapes.

2 Properties of the Curves C_k

The points where C_k segments are joined are called its *vertices*. By the iteration process every vertex of C_k is also a vertex of any C_{k+m} and hence is in K. Every vertex has a *type* which describes the direction change of the segment after it with respect to the segment before it. For two consecutive segments in C_k, if the directions of the segments before and after the vertex are α and β, respectively, then the type of

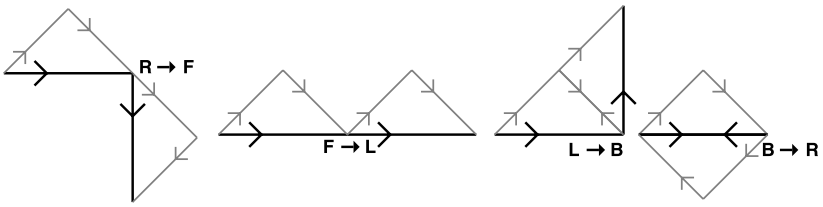

Fig. 4 The change of vertices type after one iteration

the vertex is $\beta - \alpha$. In C_{k+1} the segment before that vertex is the second segment out of the two that replace the C_k segment before it, and hence its direction is $\alpha - \pi/4$, while the segment after that vertex is the first segment out of the two that replace the C_k segment after it, and hence its direction is $\beta + \pi/4$. The type of that C_{k+1} vertex is thus $(\beta + \pi/4) - (\alpha - \pi/4) = (\beta - \alpha) + \pi/2$. The type of a vertex changes by a right angle after every iteration, and after four iterations it returns to the same type.

There are 2^{k-1} new vertices in C_k, one for every segment of C_{k-1}. The type of all of those new vertices is $\pi/2$ to the right since a C_{k-1} segment is replaced by two C_k segments to its left. There are thus only four types denoted by R for a turn to the right, F for continuing forward, L for a turn to the left, and B for a turn backward. As demonstrated in Fig. 4, a vertex created with type R in C_k has type F in C_{k+1}, type L in C_{k+2}, type B in C_{k+3}, and it returns to type R in C_{k+4}. Every vertex thus goes through a cyclic change of type with period 4 along the sequence of iterations. A vertex created in C_k is R type in C_{k+4m}, F type in C_{k+4m+1}, L type in C_{k+4m+2}, and B type in C_{k+4m+3} for any nonnegative integer m. The type of a vertex with type X that was created in C_{k-m} is denoted by $X^{[k-m]}$.

At one of the ends of any C_k segment there is a vertex with type $R^{[k]}$. The vertex at the other end was created by C_{k-m} for some $m > 0$. If two C_k segments overlap, they must have opposite directions because if two overlapping segments have the same direction, then at the end where the vertices with type $R^{[k]}$ are, there are two other overlapping segments with the same direction. This could happen only if there were two overlapping segments with the same direction in C_{k-1}. Continuing backward along the iterations sequence and repeating this argument would lead to the existence of overlapping segments pair with the same direction in any C_{k-m}. However, C_0 (and also C_1, C_2, and C_3) do not have overlapping segments at all, and hence there are no overlapping segments with the same direction in any C_k. Thus, no more than two segments can overlap because a third would have the same direction as one of them. For the rest of this paper, such an overlapping segments pair is referred to as an OSP. Another corollary of this is that no more than four vertices are located at the same point.

Since all the segments of C_k have the same length and all the turns at the vertices are multiples of right angles, all the segments of C_k are on the sides of squares of a lattice of squares tiling $\mathbb{R}^2$. These squares are referred to as the C_k *squares*. All the new vertices created by the next iteration are at centers of those squares and the C_{k+1} squares are obtained by the diagonals of the C_k squares. Hence, all the vertices located at one point were created by the same iteration as R type and thus have the same type after any number of additional iterations.

If there are vertices on the four corners of a C_k square, then the vertices on two opposite corners were created by C_k at centers of two adjacent C_{k-1} squares and thus have type R. The other two opposite corners are at the two ends of one side of a C_{k-1} square, and if there was a C_{k-1} segment on it, on one of its ends there would be a vertex created as R by C_{k-1} and thus would have type F in C_k. Hence, the vertices on two opposite corners of a C_k square are $R^{[k]}$ and on one of the other corners $F^{[k-1]}$. The vertex at the last corner was created by some iteration up to C_{k-2}.

Once the types of the vertices in a neighborhood are known, one can determine which segments are in the same path within that neighborhood. The segments in the same path either all exist or all are absent.

3 The Shapes of Interior Components

Let P be the reflection through the line perpendicular to C_0 at its center. Then P^2 is the identity, and since the fixed points of f_0 and f_1 are at the ends of C_0 and their rotation angles are opposite, $Pf_0P = f_1$ and $Pf_1P = f_0$, and thus

$$P(K) = Pf_0(K) \cup Pf_1(K) = Pf_0P^2(K) \cup Pf_1P^2(K) = f_1P(K) \cup f_0P(K)$$

and since the attractor of the iterated function system $\{f_0, f_1\}$ is unique [5], we have $P(K) = K$. Hence, P is a symmetry of the Levy dragon, and thus for every shape of interior component, the reflected shape also is a shape of an interior component. We consider such a pair of reflected shapes as one shape.

To find the shapes of the interior components, we start with the concept of a covered triangle, as demonstrated in Fig. 3(c), and transfer it to the segment of C_k so that the hypotenuse of the covered triangle is on it and the triangle is to its left. Thus, the minimal configuration for a covered segment is as in Fig. 5(a) for segment s there. It includes seven OSPs and one single segment, which is the hypotenuse of the triangle that intersects the covered triangle only at its right angle vertex. The opposite segment to a covered segment is almost covered, missing only this last single segment. Since there is an R vertex at one of the ends of this single segment because of the existence of one of the segments in the OSPs perpendicular to the single segment, the segment opposite to it must also exist. Also, because there is an R vertex at the end of one of the two OSPs to the right of segment s, there is a segment antiparallel to s there too. Thus, the minimal configuration for a covered segment s is as in Fig. 5(b).

The significance of covered segments for the purpose of finding the shapes of the interior components is that if a C_k segment is covered, the two C_{k+1} segments that are opposite to the two segments that replace it are also covered. See Fig. 5(c), where the C_{k+1} segments (in gray) that replace the C_k segments (in black) are shown, and segments r and t are covered since s is covered. Thus, the $F^k(T)$ triangle to the left of the covered segment is tiled by two covered $F^{k+1}(T)$ triangles. Continuing to the next iterations, for any nonnegative integer m, this triangle is tiled by 2^m triangles of $F^{k+m}(T)$; hence a covered triangle is a subset of K, and its interior is a subset of the interior of K.

We say that two $F^k(T)$ triangles are edge connected when they have a common edge. The interior of the union of a set of edge connected covered triangles is in the

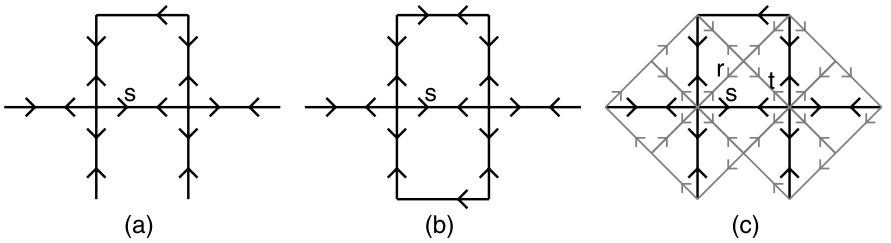

Fig. 5 (**a**) The segments configuration of a covered segment s. (**b**) The necessary extra segments. (**c**) C_{k+1} segments r and t are covered since C_k segment s is covered

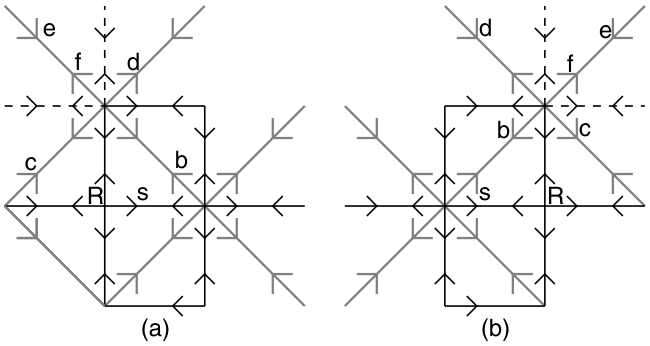

Fig. 6 The two configurations of a C_k segment s originally covered since C_{k-1} segment b is not covered

same interior component of K. The buildup of a component of the interior of K during successive iterations of $F^k(T)$ must start with the appearance after some iteration of a set of edge connected covered triangles that are not edge connected to any covered triangle generated in previous iterations. Such a seed of an interior component grows into its final shape as in the next iterations there are covered triangles edge connected to it. Finding covered triangles will thus not serve our purpose since they might be tilling a triangle that was already covered in previous iterations. Therefore we define the concept of an *originally covered segment* for a triangle that is not a subset of a covered triangle.

Definition 3.1 A C_k segment is originally covered if it is covered and the opposite segment is one of the two segments that replace a C_{k-1} segment that is not covered.

Figures 6(a) and (b) show the two configurations for a C_k covered segment s (in black) with the type $R^{[k]}$ vertex at the beginning and at the end of s, four more C_k segments in dashed lines and the segments that must be in C_{k-1} for those C_k segments to exist (in gray). The four C_{k-1} segments denoted with c, d, e, and f must exist if the C_k segments in dashed lines exist. Segment b in both cases is the C_{k-1} segment that must be not covered in order that segment s will be originally covered. For b to be not covered, at least one of the four segments c, d, e, and f must be absent in C_{k-1}, and thus at least one of the four segments with dashed lines is absent in C_k.

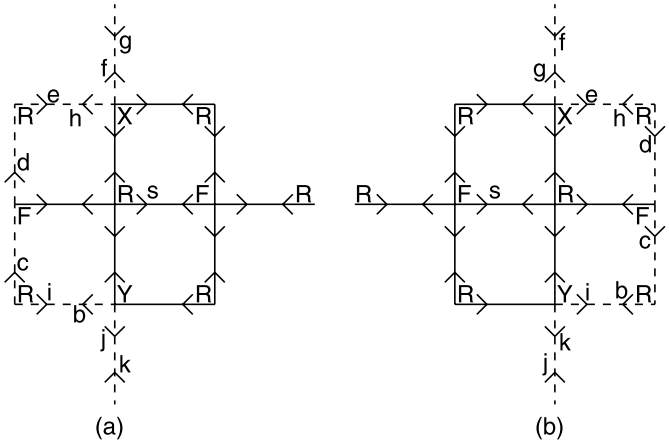

Fig. 7 The two minimal configurations of an originally covered segment

Lemma 3.2 *A C_k originally covered segment has a vertex with type $F^{[k-1]}$ at one of its end points.*

Proof Let the C_k originally covered segment be s in Figs. 6(a) and (b). Consider the C_k square to the left of s. As any C_k square, it has two $R^{[k]}$ vertices on two opposite corners and an $F^{[k-1]}$ vertex on one of the other two corners. In both cases, Figs. 6(a) and (b), the F vertex cannot be at the corner intersected by the four C_k segments with dashed lines, since if it does, all those four segments are in paths of the minimal configuration for s to be covered, hence all of them exist, and then s is not originally covered. Thus, the $F^{[k-1]}$ vertex must be on the last corner, which is an end point of segment s in both cases. □

By the same argument, also the OSP collinear with s at its R end has an $F^{[k-1]}$ vertex at its other end. The minimal two configurations of an originally covered segment is demonstrated in Figs. 7(a) and (b). The points at the ends of the OSPs perpendicular to s at its R end are denoted X and Y (we use those for the vertex and its type).

Proposition 3.3 *The segment opposite to an originally covered segment is covered. If it is originally covered, then there are only three possible configurations*:

- $X = B, Y = L$
- $X = L, Y = B$
- $X = L, Y = L$

The segments with end points at X and Y that must be absent are in one path. If it is only covered, there are only two possible configurations:

- $X = B, Y = L$
- $X = R, Y = L$

Proof The segment opposite to a covered segment is almost covered, missing only the single segment antiparallel to it on the opposite edge of the square to its left. Consider the originally covered segment s in the two cases in Figs. 7(a) and (b), and let s' be the opposite segment. Since X, Y, and the two $F^{[k-1]}$ vertices are on the four corners of a C_{k-1} square, either X or Y has type $L^{[k-2]}$.

For both cases, if Y is either R or F, then $X = L$, and the segments h and g exist since they are in the paths of segments in the covered configuration, and thus since s is originally covered, both e and f must be absent. But if Y is R or F, segment b must exist, and hence the whole path b, c, d, e must exist. Hence, Y is neither R nor F. Thus, Y is either B or L, and in both cases the one segment needed to make s' covered must exist, hence s' is covered.

Thus, if $X = L$, s' is originally covered, and either $Y = L$ or $Y = B$. If $X \neq L$, then $Y = L$, and if s' is originally covered, then segments i and j exist and segments k and b are absent. Hence, the path that includes segments b, c, d, and e is absent. But if $X = R$ or $X = F$, segment e exists, hence X can only be B.

The path that includes segments b, c, d, and e is absent in both cases, and we refer to it in these cases as the *forbidden path*.

If segment s is originally covered while s' is only covered, then two of the segments e, f, g, and h must be absent while all the four segments i, b, j, and k must exist. Since segment b exists, all the path b, c, d, e exists. If $X = L$, then h and g exist, and thus e and f must be absent, hence $X \neq L$. Also, $X \neq F$ since then all four segments exist, hence X is either B or R. Since $X \neq L$, we have $Y = L$. □

We name the three possible configurations of an OSP with the two segments originally covered by the types appearing in clockwise order around the covered area; hence we refer to the three possibilities above as the LB, BL, and LL configurations, respectively.

By Proposition 3.3 an originally covered segment can never be part of the boundary of an interior component. The hypotenuse of an originally covered $F^k(T)$ triangle is thus never on the boundary of an interior component, and only the two short edges of such a triangle can be part of the boundary. The following proposition characterizes the segments that form the boundary of covered sets.

Proposition 3.4 *If a segment is covered and the opposite segment is not covered, then those segments are on the boundary of the covered set which includes the covered triangle to the left of the covered segment.*

Proof The configuration for such an OSP in C_k with one segment covered and the other not covered is demonstrated in Fig. 5(a), where segment s is the covered segment, and the opposite segment is not covered only because one segment is absent. In C_{k+2} every C_k segment is replaced by a C_2 to its left. On every half of segment s and its opposite, there is a C_{k+2} OSP where the segment with the same direction as s is covered while the opposite segment is not covered. Thus, for all $p > 0$, in C_{k+2p} on segment s and its opposite there are 2^p OSPs with one segment covered and one not covered, so all the $F^{k+2p}(T)$ triangles with hypotenuse on s are not covered; hence s is on the boundary of the covered area. □

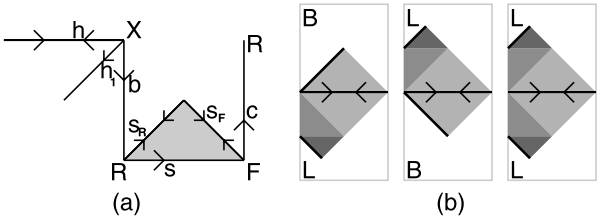

Fig. 8 (**a**) The state of segments s_R and s_F replacing an originally covered segment s. (**b**) The three stages of development of covered area starting with an originally covered OSP

Lemma 3.5 *From the two C_{k+1} segments that replace an originally covered C_k segment s, one is either originally covered or not covered, while the other is either covered or not covered depending on whether the segment opposite to s is also originally covered or only covered and on the type X at the end of the OSP perpendicular to s at its R end.*

Proof Consider Fig. 8(a). Segment s is a C_k originally covered segment that starts at the R vertex and ends at the F vertex. The gray triangle is the $F^k(T)$ triangle thus covered. Segments s_R and s_F are the two C_{k+1} segments that replace s. By Lemma 3.2, since s_R starts at an $F^{[k]}$ vertex and ends at an $R^{[k+1]}$ vertex, it can be originally covered in C_{k+1}, while s_F ends at an L vertex, and hence it cannot be originally covered.

The segment opposite to s_R is covered because s is covered, and therefore s_R is almost covered, and it is covered if the C_{k+1} segment h_1 exists and not covered if h_1 is absent. For s_R to be originally covered, the C_k segment b must be not covered. Since s is originally covered, two segments at the X end of b are absent, and thus segment b is not covered; so if s_R is covered, it is originally covered. For segment h_1 to exist in C_{k+1}, segment h must exist in C_k. By Proposition 3.3, since s is originally covered, the opposite segment is covered, and if it is originally covered, then either $X = L$, h exists, and s_R is originally covered or $X = B$, h is absent, and s_R is not covered, hence by Proposition 3.4 it is a boundary segment. If the segment opposite to s is only covered, then by Proposition 3.3 either $X = B$, h exists, and s_R is originally covered or $X = R$, h is absent, and s_r is a boundary segment.

Since s_F cannot be originally covered, either it is not covered and part of the boundary of the interior component or it is covered. It can only be covered if the C_k segment c is covered. If c is covered, it is originally covered because of the two segments that are absent at X since s is originally covered.

In case s starts at the F vertex and ends at the R vertex, the same arguments lead to the same results, only s_R is the second of the two segments replacing s, while s_F is the first. □

Theorem 3.6 *A C_k OSP with the two segments originally covered develops up to C_{k+2} into one out of three covered shapes in $F^{k+2}(T)$ depending on whether it is an LB, BL, or LL.*

Proof The covered shape for the OSP of two C_k originally covered segments is a square tiled by two $F^k(T)$ triangles (lighter gray areas in Fig. 8(b)). By Lemma 3.5,

if $X = L$, then on an edge of that square there is a C_{k+1} OSP with one originally covered segment and one covered segment, so the covered shape grows by an $F^{k+1}(T)$ triangle (darker gray areas in Fig. 8(b)). This happens once for an LB or BL and twice for LL. If $X = B$, that C_{k+1} segment is a boundary segment of the covered shape, so for an LB or BL, one edge of the square is part of the boundary (solid black lines in Fig. 8(b)). On the other two edges of the covered square, either the OSP has one covered segment and one not covered, so it is a boundary segment, or both are covered when there is another C_k originally covered segment perpendicular to the originally covered OSP at its F end.

For the C_{k+1} OSP with one covered segment and one originally covered, when $X = L$, the R vertices are at the beginning of the originally covered one, hence its X point is at the same point as for the C_k originally covered OSP, only in C_{k+1} the type turns to $X = B$. By Lemma 3.5 again on one edge of the $F^{k+1}(T)$ triangle that was added, there is a C_{k+2} OSP with one segment covered and the second originally covered, hence the covered shape grows by an $F^{k+2}(T)$ triangle (the darkest gray areas in Fig. 8(b)). The C_{k+2} OSP on the other edge either has one covered segment and one not covered, so it is a boundary segment, or both are covered when there is another C_{k+1} originally covered segment perpendicular to the C_{k+1} originally covered segment at its F end.

Finally for the C_{k+2} OSP with one covered segment and one originally covered, its X point is again at the same point, only in C_{k+2} the type turns to $X = R$. By Lemma 3.5, on one edge of the $F^{k+2}(T)$ triangle that was added, there is a C_{k+3} OSP with one segment covered and the second not covered, hence it is a boundary segment. The C_{k+3} OSP on the other edge either has one covered segment and one not covered, so it is a boundary segment, or both are covered when there is another C_{k+2} originally covered segment perpendicular to the C_{k+2} one at its F end. This originally covered segment exists if there is another C_k originally covered segment perpendicular to the originally covered OSP at its F end. Thus, the collinear C_{k+1} and C_{k+3} segments are either both boundary segments or both covered. □

To determine the possible interior components shapes, we now first explore the possible seeds of covered areas and then their possible growth patterns.

Theorem 3.7 *The possible C_k configurations for the initial edge connected set of covered $F^k(T)$ triangles of an interior component include only two configurations with one originally covered OSP, four configurations with two originally covered OSPs, and two configurations with four originally covered OSPs.*

Proof The first covered triangles of an interior component that appear in C_k are not edge connected to triangles that were covered before; hence by Proposition 3.3 they must appear only in OSPs with both segments originally covered.

Consider Fig. 9. It shows the C_k segments configuration for an LB originally covered OSP with segments denoted by s and b. The square that has the B and L vertices on two adjacent corners and the F end of the originally covered OSP at its center is a C_{k-2} square; hence the type at the corner opposite the L is another L. The type at the last corner is denoted by Z. The path of forbidden segments is marked

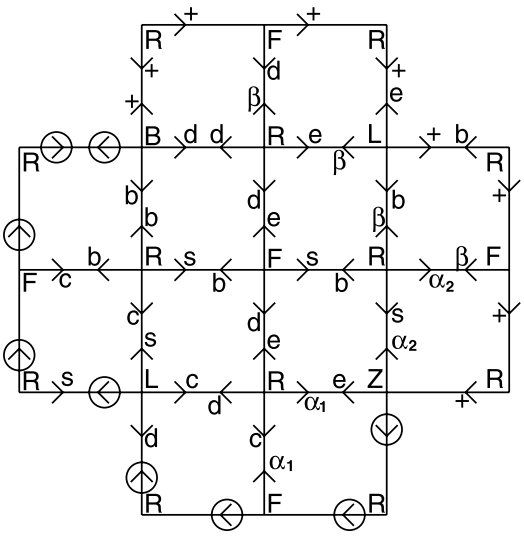

Fig. 9 The segments configuration of an LB originally covered OSP and the three possible OSPs with edge connected covered squares

with circled arrows, and it extends up to the point Z. There is also a path of segments denoted with a $+$ sign which extends up to Z. All the segments in the minimal LB configuration are in five paths, and all the segments in one path are denoted by the same labels s, b, c, d, and e. Also segments in three additional paths are denoted by α_1, α_2, and β. The segments in the $+$ path and the α_1, α_2, and β paths are not in the minimal configuration of the LB and hence may exist or be absent.

The covered area for an originally covered OSP is a square. For another originally covered OSP to be with a covered square edge connected to this square, it must be an OSP perpendicular to the first with a common end. By Lemma 3.2 such an originally covered OSP must have an $F^{[k-1]}$ at one of its ends. Hence, the only candidates are the two OSPs at the F end with segments d and e. For one of them to be originally covered, the β path must exist, while the $+$ path must be absent since it is its forbidden path. For the other to be originally covered, the α_1 and α_2 paths must exist and either $Z = B$ or $Z = L$ (its forbidden path is part of the forbidden path of the LB). The only additional possible originally covered OSP with covered square edge connected to the covered squares of those two is the OSP with segments s and b collinear with the first one with common end at its F end. For this OSP to be originally covered, the α_1, α_2, and β paths must exist, the $+$ path must be absent, and Z must be either L or B. But these are the conditions for the other two OSPs to be originally covered, hence only 1, 2, or 4 originally covered OSPs with edge connected squares can appear together.

Figure 10 demonstrates all these possibilities relative to the C_k originally covered OSPs. The gray shapes are obtained by applying Theorem 3.6 in each case, and there are solid black lines on the segments already known by Theorem 3.6 to be boundary segments. Whenever the $+$ path is optional, there is a $+$ near the B.

If the β path exists, the $+$ path must be absent, because otherwise there is a covered OSP which is not originally covered with its covered square edge connected to the

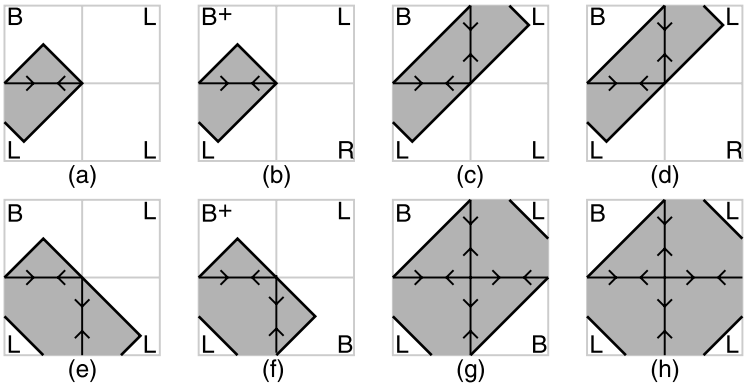

Fig. 10 The eight possible seeds of interior components

covered square of the first LB, and this is impossible for the initial appearance of covered triangles for an interior component.

$Z \neq F$ because if $Z = F$, the s path is in the forbidden path.

If $Z = R$, then α_1 is in the forbidden path, and it is absent. Then either the β path is absent, it is an LB as in Fig. 10(b), and the $+$ path is optional, or the β path exists, the $+$ path is absent, and it is an LBL as in Fig. 10(d).

If $Z = B$, then α_1 is in the e path and α_2 is in the s path, so both of them exist. If the β path is absent, then it is a BLB as in Fig. 10(f) with the $+$ path optional. If the β path exists and the $+$ path is absent, then it is an LBLBL as in Fig. 10(g). (The first L is repeated at the end for a reason that will be clear later.)

If $Z = L$, then the $+$ path is in the forbidden path, and it is absent. α_1 and α_2 are in the same path α. If both β and α are absent, it is an LB as in Fig. 10(a). If β exists and α is absent, it is an LBL as in Fig. 10(c). If β is absent and α exists, it is an LLB as in Fig. 10(e). If both β and α exist, it is an LBLLL as in Fig. 10(h).

There is no need to repeat these arguments for the configurations that start with a BL or LL since these are included within those possibilities rotated or reflected. □

The only manner in which these core shapes that are initiated in C_k and reach their final shape in C_{k+2} can grow is if in C_{k+1} there is an originally covered OSPs such that the covered squares they generate have an edge on the C_{k+2} segments on the edge of the shape which might not be a boundary segments. In Fig. 11 these OSPs for an LB, BL, and LL are denoted with g. If the g segments are covered, they are originally covered because the forbidden path prevents the relevant C_k segments from being covered. For g in all three configurations to be covered, three additional C_{k+1} segments must exist. Those segments exist in C_{k+1} if the C_k segments in path t exist. Path t exists only if the segments denoted as u_1 and v_1 exist (u_1 starts at the vertex U, and v_1 ends at the vertex V).

Since the L and F vertices in C_k turn respectively into B and L in C_{k+1}, the originally covered OSP g in an LB is a BL, in a BL it is an LB, and in an LL one LB (towards U) and one BL (towards V). By Theorem 3.6 the covered area initiated by g grows in C_{k+2} and C_{k+3} into the same basic shapes, only contracted by $1/\sqrt{2}$.

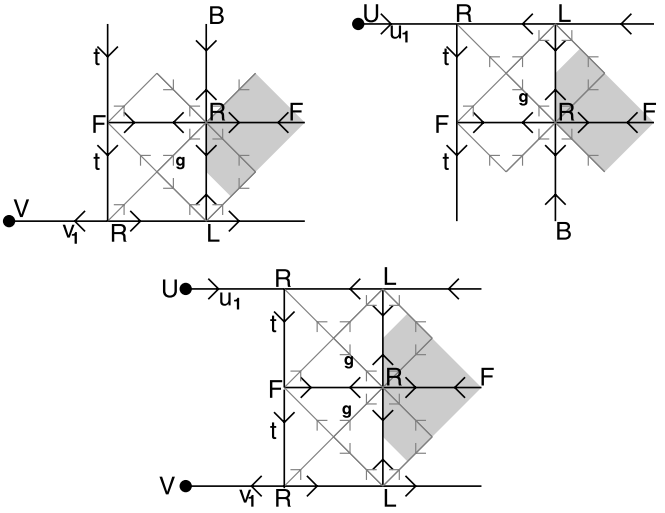

Fig. 11 The originally covered OSP g needed for growth of a LB, BL and LL

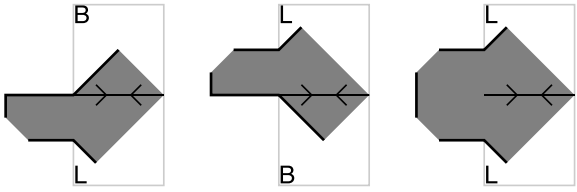

Fig. 12 First step of tail building

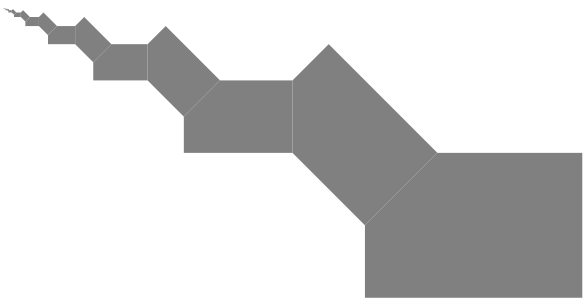

Fig. 13 A tail

Figure 12 shows the covered shapes obtained in $F^{k+3}(T)$ if u_1 and v_1 exist. In LB and BL the C_{k+1} OSP perpendicular to g at its F end cannot be covered since a C_k segment with end at the B vertex is in the forbidden path, and thus even if segments t exist, two C_{k+1} segments that must exist if that OSP is covered are absent. Hence, except for one C_{k+3} segment, all segments on the edges of the shape are boundary segments (solid black lines in Fig. 12).

This process can continue creating a tail of contracted basic shapes alternating between a BL shape and an LB shape as demonstrated in Fig. 13.

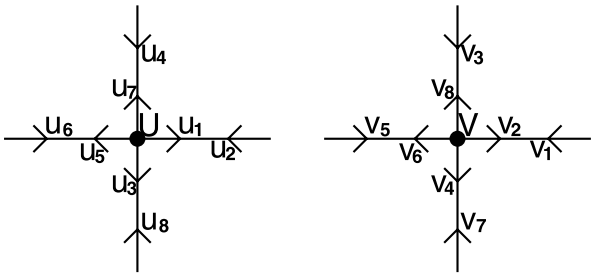

Fig. 14 Tail tip segments of U and V tail tips

We refer to the number of basic shapes in a tail as its tail length and denote the structures obtained as BnL, LnB, and Ln, mL, where n and m are the tail lengths. Every pair of consecutive basic shapes in a tail is obtained from the previous pair by a contraction by $1/2$. The points U and V are the fixed points of these contractions and the tip of the tail in case it is infinite.

For each step of this tail building to go on, the segments equivalent to u_1 and v_1 must exist. Note in Fig. 11 that for an LB (BL), the first tail shape is a BL (LB), and its U (V) point is at the V (U) point of the LB (BL). For its u_1 (v_1) segment to exist so that there will be a second basic shape in the tail, there must be a C_k segment opposite to v_1 (u_1). That segment is denoted v_2 (u_2), so the existence of v_1 and v_2 (u_1 and u_2) ensures a tail with length 2 for an LB (BL).

Every odd (even) basic shape in a tail is parallel to the first (second) one. Thus, for the p basic shape in a tail to exist, there must be a C_{k+p-1} segment parallel to v_1 or u_1 if p is odd and a C_{k+p-2} segment parallel to v_2 or u_2 if p is even. This requires the existence of C_k segments denoted by v_p or u_p obtained by rotation by p right angels counterclockwise from v_1 and u_2 and clockwise from v_2 and u_1, as demonstrated in Fig. 14.

For $p > 8$, these same C_k segments ensure the existence of the required segments, so that if the first $p-1$ shapes in a tail exist for $p = 8i + j$ if u_j or v_j exist, then the p shape in the tail exists. Thus, for any $p < 9$, if u_p (or v_p) is absent while all the segments u_1 up to u_{p-1} (or v_1 up to v_{p-1}) exist, then the tail length is finite and given by $p-1$, while if all eight segments exist, the tail length is infinite. There are thus only nine possible tail lengths for any tail, and this leads to our main result.

Theorem 3.8 *The number of shapes of the interior components of the Levy dragon is finite.*

Proof By Theorem 3.7 there is a finite number of initial sets of edge connected covered triangles (8 possible configurations). For each of those, there is a finite number of tails (up to 6). Whatever the tail tip type is, there is a finite number of possible tail lengths (9), hence the number of possible shapes is finite. □

To determine the possible interior components shapes, we first show that the possible tail lengths for the tails of an LB, BL, or LL are much more limited than those nine possible lengths. Next, the tail tip types for all tails in all the configurations obtained for different Z values in Theorem 3.7 are determined. Finally, some shapes

Table 1 Tail tip consecutive segments pairs and possible tail lengths

Tail tip type	Segment pairs	Possible tail lengths
R	$(v_1, v_8), (v_2, v_7), (v_3, v_6), (v_4, v_5)$	$0, 1, 2, 3, \infty$
F	$(v_7, v_8), (v_6, v_1), (v_3, v_4), (v_5, v_2)$	$0, 1, 2, 6, \infty$
L	$(v_5, v_8), (v_6, v_7), (v_1, v_4), (v_2, v_3)$	$0, 1, 4, 5, \infty$
B	$(v_3, v_8), (v_4, v_7), (v_5, v_6), (v_1, v_2)$	$0, 2, 3, 4, \infty$

Table 2 Possible tail lengths for a LB or BL

Tail tip type	Possible tail length	
	+ path absent	+ path exists
R	2	$3, \infty$
F	0	$1, 2, \infty$
L	Impossible	$0, 1, \infty$
B	0,4	$0, \infty$

that could exist by these conditions are proved to be impossible because of some dependencies between paths that provide tail tip segments to different tails within the same configuration.

Lemma 3.9 *The tail lengths of an LB and a BL are limited to the values in Table 2 depending on the tail tip type and existence or absence of the + path.*

Proof The eight tail tip segments are always in four pairs of consecutive segments depending on the tail tip type. The two segments of such a pair either both exist, or both are absent. Hence, there are only three possible finite nonzero tail lengths for any tail tip type shown in Table 1.

Actually the possibilities for the tail tips in a given LB or BL configuration are more limited since some of the tail tip segments are always provided by paths within the minimal configuration continued towards the tail tips. Figure 15(a) demonstrates how by using the R and F vertices within the LB configuration and C_k and C_{k-1} squares we can determine the R, F, and L vertices on paths towards the V tail tips. Thus, for the V tail tip of any LB, v_7 and v_8 always exist. In addition, v_6 is in the + path which for some configurations is forbidden and for some optional. As demonstrated in Fig. 15(b), this holds also for any BL and its U tail tip segments. Hence, the possible tail lengths for an LB or BL are those in Table 2.

□

Lemma 3.10 *The only possible tail length combinations for the double tail of an LL are $L0, 0L$, $L\infty, 1L$, $L1, \infty L$, and $L\infty, \infty L$.*

Proof As demonstrated in Fig. 15(c), continuations of paths of the minimal LL configuration provide v_7 and v_8 for the V tail tip and u_7 and u_8 for the U tail tip. U, V, and the two L vertices are on the four corners of a C_{k-2} square; hence either $U = L$

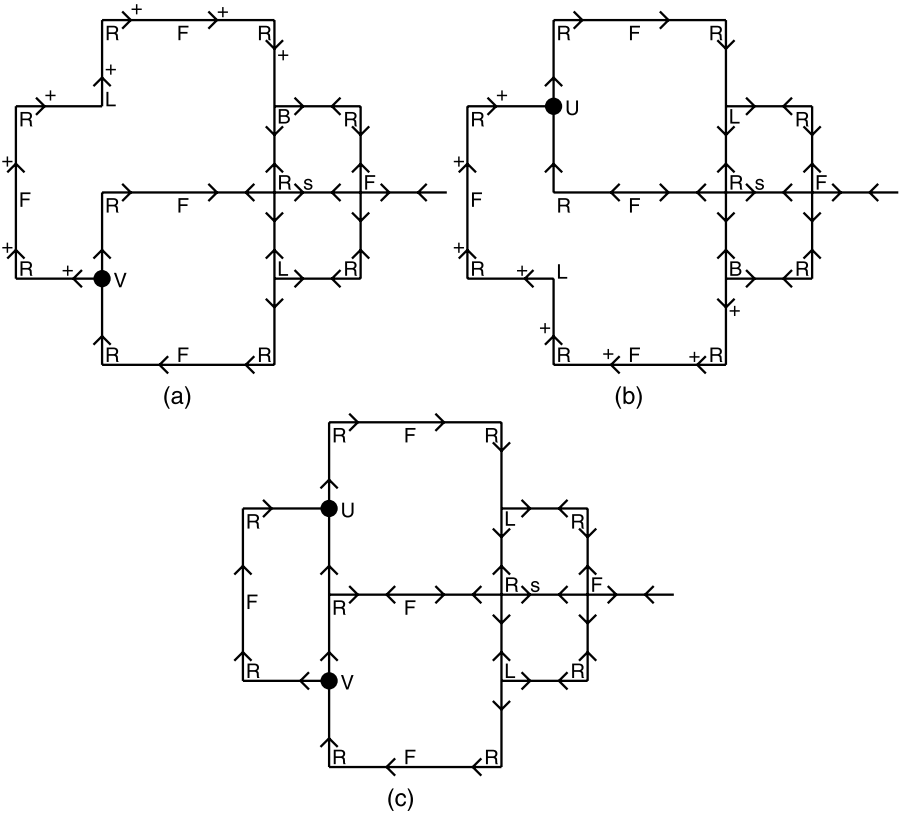

Fig. 15 Tail tip segments provided by paths in the originally covered configuration and the + path

and $V = B$, or $U = B$ and $V = L$. In the first case, u_6 and u_7 are on the same path, while in the second case, v_7 and v_6 are on the same path. But v_6 and u_6 are on the same path shown in Fig. 15(c); hence u_6 and v_6 always exist for any LL. u_1 and v_1 are on the same path; hence either both are absent and the double tail is $L0, 0L$, or both exist, in which case both tails have nonzero length. If $U = L$, $V = B$, and u_2 is absent, the double tail is $L\infty, 1L$, while if $U = B$, $V = L$, and v_2 is absent, the double tail is $L1, \infty L$. In case $U = L$ if u_2 also exists or in case $V = L$ if v_2 also exists, then the double tail is $L\infty, \infty L$. □

There are six points that are tail tips in all or some of the eight cases in Fig. 10. These six tail tips, denoted by V_1, U_1, U_2, V_2, V_3, and U_3, are emphasized in Fig. 16(a), which is the C_{k-2} configuration from which the C_k configuration in Fig. 9 is obtained by replacing every segment in Fig. 16(a) by a C_2. The segments in Fig. 16(a) are denoted by the labels of the segments that replace them in Fig. 9 and are extended up to the tail tips. The type in C_{k-2} of a vertex with type X in C_k is denoted by X^*.

Since Z is at a corner opposite a B in a C_{k-2} square, we have that if $Z \neq B$ it was created before C_{k-3}, while if $Z = B$, it might be that $Z = B^{[k-3]}$ and the other B

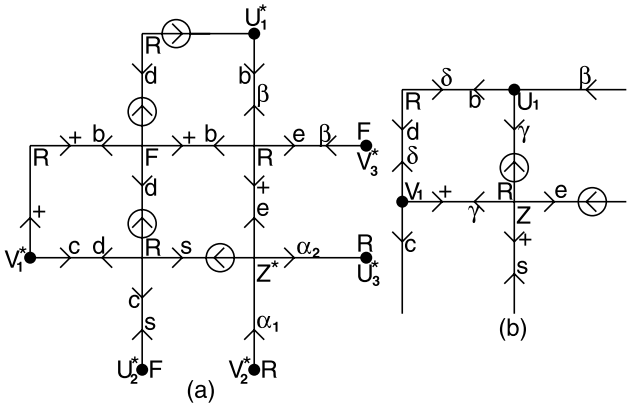

Fig. 16 (**a**) The six possible tail tips in the C_{k-2} configuration. (**b**) The C_{k-4} configuration in case $Z = R^{[k-4]}$

created before C_{k-3}. But these two possibilities lead to configurations that are related by a rotation and thus will lead to the same shapes; hence for the purpose of finding all shapes, we can assume that Z was created before C_{k-3}. Hence, $Z = R^{[k-4q]}$, or $Z = B^{[k-3-4q]}$, or $Z = L^{[k-2-4q]}$ for some integer $q > 0$.

Proposition 3.11 *The tail tip type for all the tails of the configurations in Theorem 3.7 are determined.*

Proof First, consider the case $Z = R^{[k-4]}$. Figure 16(b) shows the C_{k-4} configuration in this case. Either V_1 or U_1 is an $F^{[k-5]}$. By Theorem 3.7 the possible shapes are LB and LBL. For the LB shape, the β path is absent, but if $U_1 = F$, then β is in the b path; hence $U_1 \neq F$ and $V_1 = F$. For an LBL shape, β exists, and the $+$ path is absent. $U_1 \neq L$, so that b is not in the forbidden path, and $V_1 \neq L$, so that d is not in the $+$ path. Since at least one out of V_1 and U_1 is F, the possibilities for (V_1, U_1) are (F, F), (F, B), (F, R), (B, F), (R, F). The last two lead to configurations that are reflected versions of the previous two; hence for the purpose of determining the possible shapes, we can assume that $V_1 = F$ and U_1 is F, B, or R.

For the rest of the possibilities, since Z was created before C_{k-4}, then $V_1 = U_1 = R^{[k-4]}$. U_2, V_2, and Z are on three corners of a C_{k-2} square with an $L^{[k-2]}$ in the last corner; hence $V_2 = L^{[k-2]}$ and $U_2 = B^{[k-3]}$. Also V_3, U_3, and Z are on three corners of another C_{k-2} square with an $L^{[k-2]}$ in the last corner; hence $U_3 = L^{[k-2]}$ and $V_3 = B^{[k-3]}$. Thus, all six tail tip types are known. □

Figure 17 shows the C_{k-2} configuration with the paths extended up to the tail tips and the additional paths $\gamma, \delta, \mu, \nu, \eta$, and χ that might provide the rest of the tail tip segments.

Lemma 3.12 *If $Z = R^{[k-4]}$, then the shape $L2B$ is impossible.*

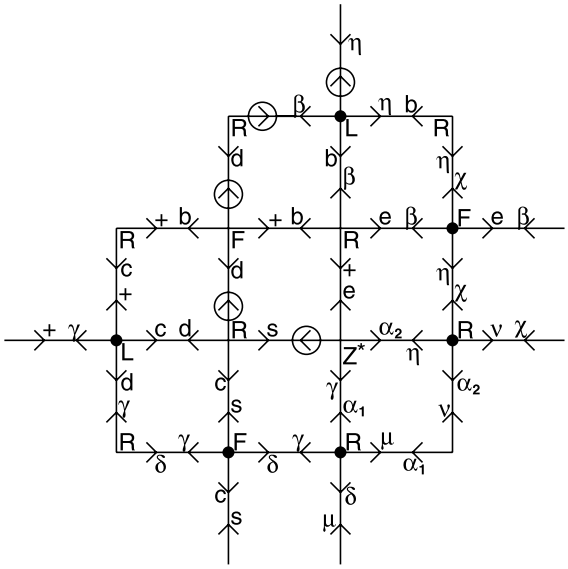

Fig. 17 The C_{k-2} configuration in case Z was created before C_{k-4}

Proof By Proposition 3.11 in this case $V_1 = F$. Two paths, γ, which provides v_2 and v_5, and δ, which provides v_3 and v_4, are added in Fig. 16(b) and extended up to U_1. If $U_1 = L$, then b is in the forbidden path, and hence $U_1 \neq L$. If γ exists, then also $U_1 \neq B$; otherwise γ is in the forbidden path. Thus, if γ exists, then $U_1 = R$, but then δ is in the same path as γ, so both of them exist. For an $L2B$ shape, γ exists and δ is absent; hence it is impossible in this case. □

Note that $L2B$ is possible in other configurations $Z = R^{[k-4q]}$ with $q > 1$ and $Z = L^{[k-2-4q]}$.

Lemma 3.13 *If $Z = B$, the shape $B0L\infty B$ is impossible.*

Proof For $B0L\infty B$ to exist, in case $Z = B$, the $+$ path must exist, but the δ path must be absent. Consider the vicinity of Z when it was created in C_{k-3-4q} obtained from its vicinity in C_k and demonstrated in Fig. 18(a) for q even and Fig. 18(b) for q odd. In both cases the square with corners at P, Q, S, and T is a C_{k-4-4q} square and hence in C_{k-3-4q} either $P = Q = F$ and one out of S and T is L, or $S = T = F$ and one out of P and Q is L. If $Q = F$, then in both cases δ is in the c path, so it always exists. If $S = T = F$, then in the even q case, if $P = L$, the β path is in the e path, but β is absent, hence $P \neq L$ and $Q = L$, and thus δ is in the γ path which is in the $+$ path, while in the odd q case, if $P = L$, then β is in the $+$ and γ path, and if the $+$ path exists, $P \neq L$ and $Q = L$, and δ is in the e path. Thus, in both cases, if the $+$ path exists, then δ exists, so $B0L\infty B$ is impossible.

□

Lemma 3.14 *If $Z = L$ the shape $L2B2L\infty$, $1L1$, ∞l is impossible.*

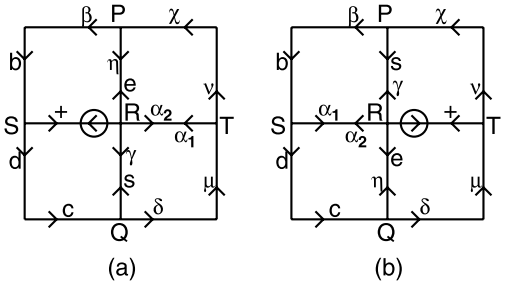

Fig. 18 The C_{k-3-4q} configurations in case $Z = B$ (**a**) q even (**b**) q odd

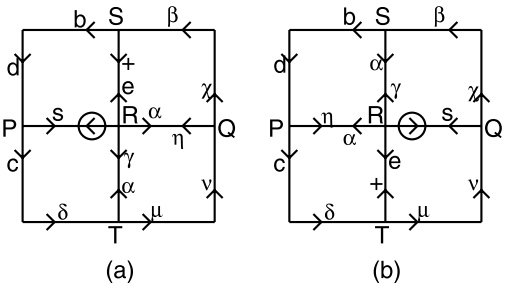

Fig. 19 The C_{k-2-4q} configurations in case $Z = L$ (**a**) q even (**b**) q odd

Proof Consider the vicinity of Z when it was created in C_{k-2-4q}, as demonstrated in Fig. 19(a) for q even and Fig. 19(b) for q odd. In both cases the square with corners at P, Q, S, and T is a C_{k-3-4q} square, and hence in C_{k-2-4q} either $P = Q = F$ or $S = T = F$. In both cases, if $T = F$, then δ and μ are in the same path, and if $Q = F$, then ν and χ are in the same path, thus it never happens that χ and δ exist while ν and μ are absent, and thus $L2B2L\infty, 1L1, \infty L$ is impossible.

□

Theorem 3.15 *Each interior component of the Levy dragon is similar to one out of the following* 23 *shapes*:

5 LB *shapes*: $L0B$, $L1B$, $L2B$, $L3B$, *and* $L\infty B$;

4 LBL *shapes*: $L0B0L$, $L2B0L$, $L4B0L$, *and* $L2B2L$;

3 LLB *shapes*: $L\infty$, $\infty L2B$, $L1, \infty L2B$, *and* $L0, 0L2B$;

3 BLB *shapes*: $B\infty L\infty B$, $B2L4B$, *and* $B0L2B$;

3 $LBLBL$ *shapes*: $L2B2L0B4L$, $L2B2L4B4L$, *and* $L2B2L0B0L$;

5 $LBLLL$ *shapes*: $L2B2L0, 0L0, 0L$, $L2B2L\infty, 1L0$, $0L$, $L2B2L\infty, \infty L0$, $0L$, $L2B2L\infty, 1L\infty, \infty L$, *and* $L2B2L\infty, \infty L\infty, \infty L$.

Proof Using all the initial configurations in Theorem 3.7 with the tail tip types determined in Proposition 3.11 and the corresponding tail lengths in Lemma 3.9 and Lemma 3.10 and removing the impossible shapes in Lemmas 3.12, 3.13, and 3.14, these 23 shapes are the only possible interior components shapes of the Levy dragon. □

These 23 possible shapes are demonstrated in Fig. 20.

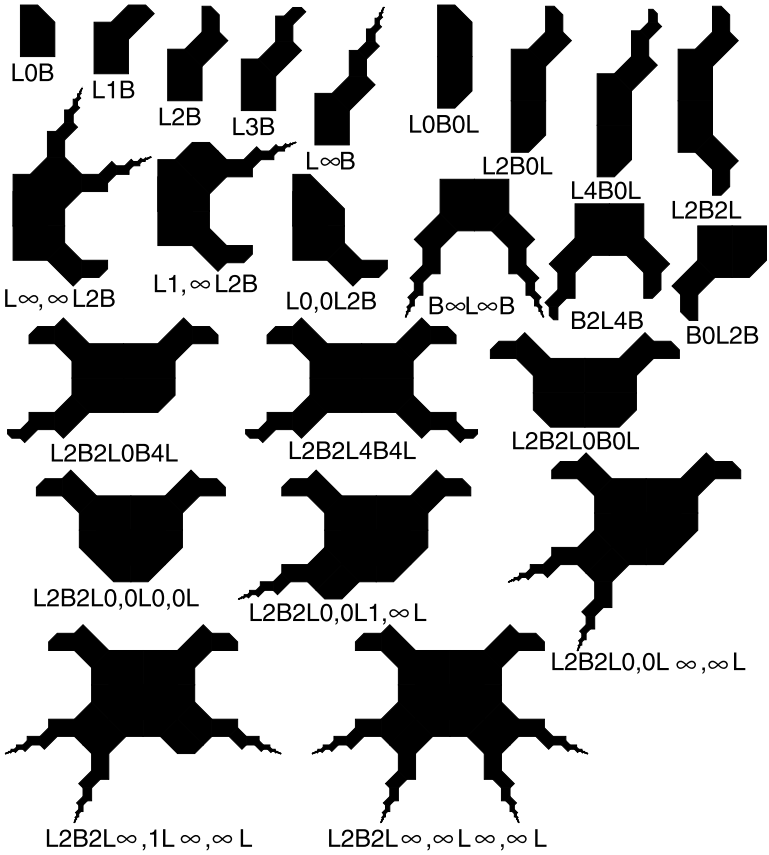

Fig. 20 The 23 possible shapes of interior components of the Levy dragon

By using a program that draws the $F^k(T)$ triangles differentiating between covered and not covered triangles one can see that all these 23 possible shapes appear. One representative of each shape is initiated up to C_{35} within distances less than $3l_{14}$ from an $L0B0L$ initiated in C_{14}.

The method of this paper can be used to determine many other geometric properties of the Levy dragon. For example, replacing existing segments by absent segments and vice versa, one can determine that the possible shapes of the holes of the Levy dragon are the same 23 shapes. By using a similar program one can see that there are holes with all those shapes. Finding those hole shapes is a much easier task than finding the interior components shapes since their configurations appear much earlier in the C_k sequence. Some of the holes are thus big enough to be seen in Fig. 1. The first one to appear in C_7 is the configuration of an $L2B2L\infty, \infty L\infty, \infty L$ hole seen in Fig. 1 at the center of the Levy dragon.

References

1. Bailey, S., Kim, T., Strichartz, R.S.: Inside the Levy dragon. Am. Math. Mon. **109**, 689–703 (2002)
2. Duvall, P., Keesling, J.: The Hausdorff dimension of the boundary of the Levy dragon. Int. J. Math. Math. Sci. **20**, 627–632 (1997)
3. Deng, D.W., Ngai, S.M.: Vertices of self-similar tiles. Ill. J. Math. **49**, 857–872 (2005)
4. Edgar, G.A.: Classics on Fractals, pp. 181–239. Addison–Wesley, Reading (1993);
5. Hutchinson, J.E.: Fractals and self similarity. Indiana Univ. Math. J. **30**, 713–747 (1981)
6. Lévy, P.: Les courbes planes ou gauches et les surfaces composé de parties semblales au tout. J. École Polytech. 227–247, 249–291 (1938)
7. Ngai, S.M., Nguyen, N.: The Heighway dragon revisited. Discrete Comput. Geom. **29**, 603–623 (2003)
8. Ngai, S.M., Tang, T.M.: Topology of connected self-similar tiles in the plane with disconnected interior. Topol. Appl. **150**, 139–155 (2005)
9. Strichartz, R.S., Wang, Y.: Geometry of self-affine tiles I. Indiana Univ. Math. J. **48**, 1–24 (1999)